Efficient delivery of meteorites to the Earth from a wide range of asteroid parent bodies

D. Vokrouhlický* & P. Farinella†

* *Institute of Astronomy, Charles University, Holešovičkách 2, 18000 Prague, Czech Republic*
† *Dipartimento di Astronomia, Università da Trieste, Trieste, Italy*

Almost all meteorites come from asteroids, but identifying their specific parent bodies, and modelling their transport to the Earth, has proved to be difficult[1,2]. The usual model[1,3,4] of delivery through orbital resonances with the major planets[5,6] has recently been shown[7–10] to deplete the supply of meteorites much too rapidly to explain either the observed flux at the Earth, or the length of time the meteorites have spent in space (as measured by cosmic-ray exposure ages). Independently, it has been found that a force arising from anisotropically emitted thermal radiation from asteroidal fragments (the 'Yarkovsky effect') influences the fragments' orbits in important ways[11–14]. Here we report the results of a detailed model for the transport of meteorites to the Earth, which includes the Yarkovsky effect and collisional evolution of the asteroidal fragments. We find that the Yarkovsky effect significantly increases the efficiency of the delivery of meteorites to the Earth, while at the same time allowing a much wider range of asteroids to contribute to the flux of meteorites. Our model also reproduces the observed distribution[15,16] of cosmic-ray exposure ages of stony meteorites.

The Yarkovsky effect, a recoil force due to anisotropically emitted thermal radiation, strongly affects the long-term orbit evolution of Solar System bodies up to the size of small asteroids[17]. The anisotropy of the surface temperature is established as a consequence of the hemispheric absorption of the solar radiation. Its quantitative description requires a detailed physical model of the heat conduction in the body and thermal reradiation by its surface. Interplay between the rotation and revolution periods, both observed or theoretically modelled, and the heat relaxation timescale, derived from the measured material parameters of meteorites and observations of asteroids, results in a permanent acceleration along the orbit. The semimajor axis thus undergoes secular change at a speed and in a direction related to the body's size, thermal properties and rotational state[11,13,14]. Typical drift rates range from 10^{-4} to 10^{-2} AU Myr^{-1}, large enough to probably detect the Yarkovsky effect using future measurements of the near-Earth asteroid (NEA) orbits[18].

As a consequence of the Yarkovsky effect, small bodies can drift in the asteroid belt for many millions of years between their initial ejection from a sizeable parent asteroid and their eventual insertion into a resonance. Such a prolonged intermediate phase implies that meteoroids are likely to be fragmented by impacts while drifting, and several generations of such break-up events may take place. Most of the original fragments delivered from a large parent body sooner or later become evolving swarms of smaller objects, all drifting at different speeds. Only a small fraction of these fragments will hit the Earth.

To describe this complex process, we have developed a realistic statistical model, including impact events along with Yarkovsky orbital drift and resonant effects. Each potential meteoroid is characterized in our simulation by three orbital (proper) elements, plus a radius, an obliquity angle and an initial time at which it starts to be irradiated by cosmic rays. We assume that all the bodies have the same thermal parameters, in particular the surface conductivity K.

Our simulations start by ejecting from a main-belt parent asteroid a swarm of fragments with a total mass equal to that of an object 500 m in diameter. The initial ejecta, as well as the fragments generated later from subsequent break-up events, have a size distribution such that the number of bodies larger than radius R is proportional to $R^{-5/2}$; their spin axes are distributed isotropically, and the orbital elements are varied according to a power-law distribution of ejection velocities[1]. As most meteorites have preatmospheric sizes exceeding 10 cm, we always neglect in our simulations the fragments of radius less than 10 cm.

We then allow the initial swarm of about 66 million fragments to evolve by several different mechanisms that all act simultaneously. First, the semimajor axes drift according to the Yarkovsky effect, depending on the fragment's orbital elements, size, obliquity and thermal parameters[14]. Second, the obliquities change randomly at average intervals $\tau_{\rm rot} = 15\,R^{1/2}$ Myr (hereafter R is in metres) and the collisional fragmentations are assumed to appear at average intervals $\tau_{\rm dis} = 16.8\,R^{1/2}$ Myr. The two lifetimes $\tau_{\rm rot}$ and $\tau_{\rm dis}$ are computed with a simple analytical model[11,13,17], using average collisional probability and impact velocity values that are appropriate for the inner part of the asteroid belt. If a body is disrupted we consider a swarm of fragments generated as described above. The cosmic-ray exposure (CRE) age of the fragments is updated by assuming that the material lying at depths greater than 1.5 m in the parent body is shielded from cosmic rays.

When a body reaches the edge of ν_6 or 3/1 resonances with the motion of the giant planets, represented by a surface in the proper-element space (and located by numerical integrations[10]), its further dynamics is assumed to be dominated by resonant effects and planetary close encounters (making Yarkovsky perturbations negligible). These post-resonant bodies continue to undergo shattering impacts (with $\tau_{\rm dis} = 14.2\,R^{1/2}$ Myr) and the CRE ages of the fragments are updated as above until some of their final offspring hit the Earth (we then record the radius and CRE age). For each body, this is assumed to occur after a time chosen by a Monte Carlo routine according to the distribution derived in ref. 10.

The entire simulation is stopped either after about 1 Gyr of evolution, if we aim at simulating the effects of very old break-up

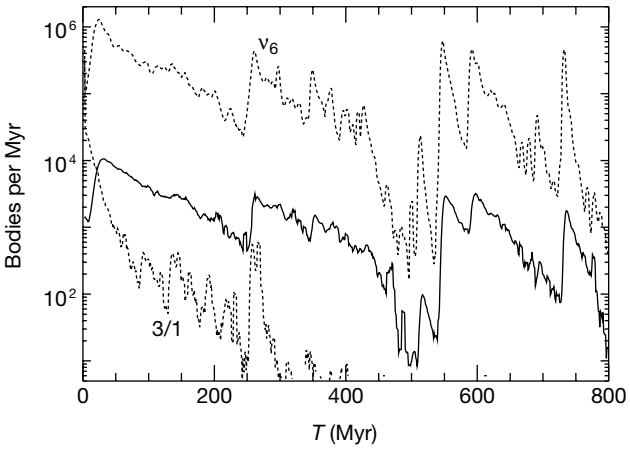

Figure 1 The expected flux of fragments from Hebe (for $K = 0.1$ W m^{-1} K^{-1}) versus time. Data is shown for the ν_6 and 3:1 resonances (dotted lines) and the Earth (full line). The flux is dominated by small ($R < 1$ m) fragments, and the large fluctuations (about a factor of 100) of the resonance fluxes are a result of secondary fragmentations of relatively large bodies into swarms of smaller ones. The flux at the Earth (that is, number of impacts) mimics the behaviour of the flux to ν_6, which is the main delivery route in this case, although it is 'smoothed out' by the chaotic character of the post-resonant orbits. We note that if the radius R_1 of the largest body in the initial distribution of ejecta were changed, the quantities plotted along the vertical and horizontal axes in this diagram would scale roughly proportional to $R_1^{5/2}$ and $R_1^{1/2}$, respectively.

events in the main belt; or after some given, shorter time span. In the former case, the resulting distribution of sizes and CRE ages also approximates the steady-state distribution for a population of meteoroids originating in many different events at random times over the simulation time span; the latter option appropriately simulates a specific, recent break-up event.

We have carried out nine 1-Gyr runs, starting from three different locations in the inner main belt, corresponding to ejecta swarms from the asteroids Vesta, Hebe and Flora (chosen both because they had been previously identified as probably meteorite parent bodies[1,2,19,20] and because they are located in different regions of the orbital-element space). As the Yarkovsky effect depends on the fragments' thermal conductivity K, we have made simulations with three widely different values of this parameter: 0.0015 $W m^{-1} K^{-1}$, as appropriate for dusty or regolith-covered surfaces[21]; 0.1 $W m^{-1} K^{-1}$, plausible for porous or fragmented rocks[21,22]; and 1 $W m^{-1} K^{-1}$, a typical value for 'bare' meteoritic rocks[22]. Every simulation has been repeated three times, with different choices of random seeds, and the results have been averaged to filter out any flukes.

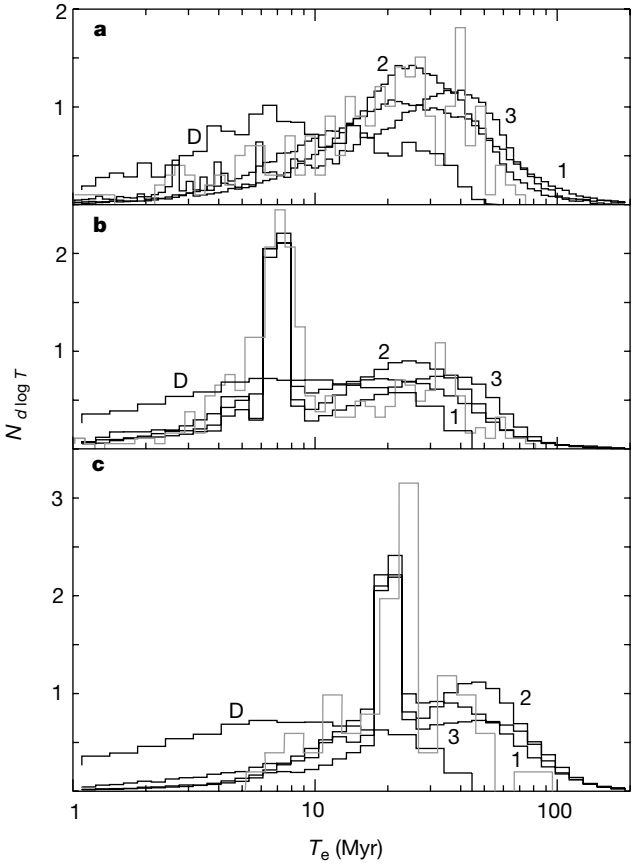

Figure 2 Comparison of the modelled and observed cosmic-ray exposure (CRE) age distributions for three different meteorite types. The data in the grey histograms is taken from refs 15 and 28. For the predictions, we show results of the direct-injection case with no Yarkovsky mobility (D histogram) and the model including Yarkovsky mobility of the meteoroids and their precursors (bold histograms). Histograms 1, 2 and 3 refer to thermal conductivity values of 0.0015, 0.1 and 1 $W m^{-1} K^{-1}$, respectively. As the ordinate represents an absolute quantity—$N_{d\log T}$: number of meteorites in a given logarithmic bin (T_e, $T_e + d\log T_e$) normalized by the total number of meteorites and the bin width $d\log T_e$—both the data and the results of our simulations were normalized independently. **a**, Assumed ejecta from asteroid Flora whose computed CRE ages are compared with the observed distribution for 240 L-chondrites. **b**, Assumed ejecta from asteroid Hebe compared with the 444 CRE ages of H-chondrites. **c**, Assumed ejecta from asteroid Vesta, compared to the CRE age data for 64 HED (howardite–eucrite–diogenite) meteorites. In all cases, the intermediate K value appears to provide the best match to the data. We note that the direct-injection scenario would always predict many more short CRE ages than are observed, and a shortage of ages between 20 and 50 Myr. Neither of these problems is present when the Yarkovsky mobility is taken into account.

The high efficiency of the Yarkovsky-driven transport mechanism, in synergy with the collisional cascade effects, is one of the unusual results from these simulations. About 40% to 90% of the initial ejecta mass always ends up in one of the two resonances within approximately the 1-Gyr time span (weakly depending on K and the starting location), compared to fractions of approximately 1% or less for fragments directly inserted in the resonances after the initial ejection event. Taking into account that only 1.18% and 0.23% of the ν_6 and 3/1 resonant particles hit the Earth[10], our results mean that the overall Earth transfer efficiency from the main belt ranges between 0.35% and 0.86%. The corresponding absolute flux depends on the production rate of ejecta. The approximately 0.6% mean Earth delivery efficiency of ejecta from main-belt asteroids is only about a factor of 10 lower than that from NEAs[23], and as the latter are at least a factor of 100 less abundant than inner-belt bodies at sizes of the order of 1 km, kilometre-sized NEAs should not be contributing a large fraction of the meteorites.

Although the supply of meteorites to our planet is eventually about the same in our model as in the classical direct-injection scenario (because the classical model largely over-estimated the number of the Earth impactors among bodies in the resonances), from another point of view our model leads to very different conclusions. For instance, our results imply that most asteroids in the inner main belt (up to $a \approx 2.7$ AU) must be relatively efficient sources of ejecta to the resonances, with limited dependence on the location of their orbit. This result differs from many previous studies that had indicated that only a small percentage of asteroids, especially those near the borders of major resonances, would contribute to the meteorite flux. Large asteroids, such as Vesta and Hebe, are likely to provide a higher yield due to their greater cross-section[13], but it is possible that this is compensated by their higher escape velocities and the increasing number of asteroids at smaller and smaller sizes. A better knowledge of the asteroid/projectile size distribution and the typical ejecta speed is required to assess the relative importance of parent asteroids of different sizes[1,13].

Figure 1 shows that the average Earth flux from a single event decreases with respect to the early values very slowly, over times of several hundred Myr (several times longer than τ_{dis} for the largest bodies in the evolving swarm). This is consistent with the evidence that a currently abundant meteorite type, the L-chondrites, underwent a large-scale beak-up event about 500 Myr ago, as indicated by their ^{39}Ar–^{40}Ar ages[24]. Note that the flux from any single source event fluctuates significantly, which might explain the evidence from fossil chondritic meteorites that the Earth flux was much higher some 480 Myr ago[25]. However, any drastic fluctuations in the meteorite flux or its compositional mixture over timescales up to about 10 Myr is prevented by the chaotic nature of the post-resonant orbits, and by the fact that at any given time the Earth is hit by fragments produced by many distinct ejection events from different parent asteroids.

Our model allows us to predict the distribution of CRE ages for the Earth-hitting objects from different parent asteroids and with different values of K (Fig. 2). We note that our simulated meteorites on average have undergone two to five break-up events during the trip, suggesting that "complex" CRE histories[15,26,27], recording variable exposure geometries, should be commonplace. The interplay of the slow transport process and the relatively frequent fragmentations also means that in a steady-state case most CRE ages range from about 10 to 50 Myr, in agreement with the data for stony meteorites. CRE ages shorter than about 5 Myr are quite rare, and this is an important argument that favours our model over the direct injection scenario, which cannot explain why such 'young' fragments are seldom observed.

Our results indicate that the $K = 0.1\,\mathrm{W\,m^{-1}\,K^{-1}}$ Flora case provides a relatively good fit to the observed CRE age distribution for the most common type of stony meteorite falls, the L-chondrites (about 40% of all the falls). Flora is the largest body of a very numerous, broad 'clan' of asteroids located at $a \approx 2.2$ AU, just out of ν_6, so our results would suggest that this entire region of the belt is a plausible source for the L-chondrites.

It is well known that for some meteorite types the observed CRE ages show distinct clusters or peaks. In the case of the H-chondrites[28], about half (some 15% of all meteorite falls) have CRE ages of 7 ± 1 Myr. Our model cannot reproduce these features by assuming that they are the consequence of relatively recent (but otherwise 'normal') fragment production events, because the flux from any given event lasts for hundreds of Myr, with a very slow decline as a function of time. Therefore it would be impossible to get a large fraction of the meteorites associated with a single recent event unless it were of an unusual magnitude.

To test this possibility, we ran our model again for the case of Hebe, a plausible parent body of the H-chondrites[19,20]. We stopped the simulation after only 8 Myr and selected the bodies hitting the Earth in the last 1 Myr of this short simulation. We then superimposed these simulated discrete-event CRE ages to the steady-state distribution predicted by the model for meteorites from Hebe, with weights determined by a least-squares best fit to the data (about 0.3 and 0.7, respectively). The agreement is quite good, although there is some evidence for a second unmodelled peak at about 33 Myr.

We applied the same technique to compare the model CRE ages obtained in the case of Vesta with the data for the HED (howardite–eucrite–digenite) meteorites[16] (spectral and mineralogical evidence suggests this large asteroid as the parent body[8,29]). Here the prominent 23 Myr peak has been fitted by taking 0.2 and 0.8 weights for the discrete-event and the steady-state distributions. Although the fit of the model to the data is again good, the CRE ages longer than 50 Myr and shorter than 5 Myr are overabundant in the model histogram. This is possibly due to our simplified method of resetting the CRE clock after secondary fragmentations, which are more numerous (typically 4–5) for Vesta's ejecta because the source body is relatively far from the resonances. However, in this case the statistics are not as good, because only a small number of the CRE age data are available. □

Received 29 April 1999; accepted 9 August 2000.

1. Farinella, P., Gonczi, R., Froeschlé, Ch. & Froeschlé, C. The injection of asteroid fragments into resonances. *Icarus* **101,** 174–187 (1993).
2. Wetherill, G. W. & Chapman, C. R. in *Meteorites and the Early Solar System* (eds Kerridge, J. F. & Matthews, M. S.) 35–67 (Univ. of Arizona Press, Tucson, 1988).
3. Greenberg, R. & Chapman, C. R. Asteroids and meteorites—Parent bodies and delivered samples. *Icarus* **55,** 455–481 (1983).
4. Wetherill, G. W. Asteroidal source of ordinary chondrites. *Meteoritics* **20,** 1–22 (1985).
5. Wisdom, J. Meteorites may follow a chaotic route to Earth. *Nature* **315,** 731–733 (1985).
6. Scholl, H. & Froeschlé, Ch. The ν_6 secular resonance region near 2 AU: A possible source of meteorites. *Astron. Astrophys.* **245,** 316–321 (1991).
7. Farinella, P. *et al.* Asteroids falling into the Sun. *Nature* **371,** 314–317 (1994).
8. Migliorini, F. *et al.* Vesta fragments from ν_6 and 3:1 resonances: Implications for V-type NEAs and HED meteorites. *Meteor. Planet. Sci.* **32,** 903–916 (1997).
9. Gladman, B. J. *et al.* Dynamical lifetimes of objects injected into asteroid belt resonances. *Science* **277,** 197–201 (1997).
10. Morbidelli, A. & Gladman, B. Orbital and temporal distributions of meteorites originating in the asteroid belt. *Meteor. Planet. Sci.* **33,** 999–1016 (1998).
11. Farinella, P., Vokrouhlický, D. & Hartmann, W. K. Meteorite delivery via Yarkovsky orbital drift. *Icarus* **132,** 378–387 (1998).
12. Hartmann, W. K. *et al.* Reviewing the Yarkovsky effect: New light on the delivery of stones and irons from the asteroid belt. *Meteor. Planet. Sci.* **34,** A161–A168 (1999).
13. Bottke, W. F., Rubincam, D. P. & Burns, J. A. Dynamical evolution of main belt meteoroids: Numerical simulations incorporating planetary perturbations and Yarkovsky thermal forces. *Icarus* **145,** 301–331 (2000).
14. Vokrouhlický, D. A complete linear model for the Yarkovsky thermal force on spherical asteroid fragments. *Astron. Astrophys.* **344,** 362–366 (1999).
15. Marti, K. & Graf, T. Cosmic-ray exposure history of ordinary chondrites. *Annu. Rev. Earth Planet. Sci.* **20,** 221–243 (1992).
16. Welten, K. C. *et al.* Cosmic-ray exposure ages of diogenites and the recent collisional history of the HED parent body/bodies. *Meteor. Planet. Sci.* **32,** 891–902 (1997).
17. Farinella, P. & Vokrouhlický, D. Semimajor axis mobility of asteroidal fragments. *Science* **283,** 1507–1510 (1999).
18. Vokrouhlický, D., Milani, A. & Chesley, S. R. Yarkovsky effect on small near-Earth asteroids: Mathematical formulation and examples. *Icarus* (in the press).
19. Migliorini, F. *et al.* Surface properties of (6) Hebe: A possible parent body of ordinary chondrites. *Icarus* **128,** 104–113 (1997).
20. Gaffey, M. J. & Gilbert, S. L. Asteroid 6 Hebe: The probable parent body of the H-type ordinary chondrites and the IIE iron meteorites. *Meteor. Planet. Sci.* **33,** 1281–1295 (1998).
21. Presley, M. A. & Christensen, P. R. Thermal conductivity measurements of particulate materials. *J. Geophys. Res.* **102,** 6535–6550 (1997).
22. Yomogida, K. & Matsui, T. Physical properties of ordinary chondrites. *J. Geophys. Res.* **88,** 9513–9533 (1983).
23. Gladman, B., Michel, P. & Froeschlé, Ch. The near-Earth object population. *Icarus* **146,** 176–189 (2000).
24. Haack, H., Farinella, P., Scott, E. R. D. & Keil, K. Meteoritic, asteroidal and theoretical constraints on the 500 Ma disruption of the L chondrite parent body. *Icarus* **119,** 182–191 (1996).
25. Schmitz, B., Peucker-Ehrenbrink, B., Lindström, M. & Tassinari, M. Accretion rates of meteorites and cosmic dust in the early Ordovician. *Science* **278,** 88–90 (1997).
26. Wetherill, G. W. Multiple cosmic-ray exposure ages of meteorites. *Meteoritics* **15,** 386–387 (1980).
27. Herzog, G. F. *et al.* Complex exposure histories for meteorites with "short" exposure ages. *Meteor. Planet. Sci.* **32,** 413–422 (1997).
28. Graf, T. & Marti, K. Collisional history of H chondrites. *J. Geophys. Res.* **100,** 21247–21263 (1995).
29. Binzel, R. P. & Xu, S. Chips off of asteroid 4 Vesta—Evidence for the parent body of basaltic achondrite meteorites. *Science* **260,** 186–191 (1993).

Acknowledgements

This Letter is dedicated to the memory of P.F., who passed away on 25 March 2000. Our understanding of the role of the Yarkovsky effect in the history of the Solar System is only one of many contributions by P.F. to modern planetology. We thank J. A. Burns and C. R. Chapman for comments on the manuscript.

Correspondence and requests for materials should be addressed to D.V. (e-mail: vokrouhl@mbox.cesnet.cz).

Trapping and emission of photons by a single defect in a photonic bandgap structure

Susumu Noda, Alongkarn Chutinan & Masahiro Imada

Department of Electronic Science and Engineering, Kyoto University, Kyoto 606-8501, Japan

By introducing artificial defects and/or light-emitters into photonic bandgap structures[1,2], it should be possible to manipulate photons. For example, it has been predicted[2] that strong localization (or trapping) of photons should occur in structures with single defects, and that the propagation[3,4] of photons should be controllable using arrays of defects. But there has been little experimental progress in this regard, with the exception of a laser[5] based on a single-defect photonic crystal. Here we demonstrate photon trapping by a single defect that has been created artificially inside a two-dimensional photonic bandgap structure. Photons propagating through a linear waveguide are trapped by the defect, which then emits them to free space. We envisage that this phenomenon may be used in ultra-small optical devices whose function is to selectively drop (or add) photons with various energies from (or to) optical communication traffic. More generally, our work should facilitate the development of all-optical circuits incorporating photonic bandgap waveguides and resonators.

The photonic bandgap (PBG) structure considered in this work is a two-dimensional PBG slab with a triangular lattice structure as shown in Fig. 1a. The structure makes use of the effect of a two-dimensional PBG to confine the light in the in-plane direction for transverse-electric (TE)-like mode, and large refractive index